JOURNAL OF GEOPHYSICAL RESEARCH, VOL. 103, NO. D21, PAGES 28,337–28,346, NOVEMBER 20, 1998

Spurious aerosol measurements when sampling from aircraft in the vicinity of clouds

R. J. Weber,[1] A. D. Clarke,[2] M. Litchy,[2] J. Li,[2] G. Kok,[3]
R. D. Schillawski,[3] and P. H. McMurry[4]

Abstract. Extensive airborne measurements of aerosol particles in a pristine marine region were made during the first Aerosol Characterization Experiment (ACE 1) from November 15 to December 14, 1995. During this study, high concentrations of condensation nuclei (CN) were frequently observed both near and within clouds. Near clouds, in the absence of liquid water, *Clarke et al.* [1998] have reported that high CN levels were from new particle formation by homogeneous nucleation. Here we show, however, that within clouds, elevated CN concentrations were not authentic, but instead a sampling artifact, likely related to fragmentation of cloud drops impacting the aerosol inlet. By themselves, these fragments were often indistinguishable from ambient particles. Spurious CN from fragmenting droplets were observed at temperatures down to roughly -20°C and spanned a broad size range, with diameters down to 3 nm. Comparison of two different sized isokinetic aerosol inlets showed that inlets with smaller openings produce higher droplet fragment concentrations. The mechanism for producing these particles is not completely understood. Although fragmentation appeared to be the primary mechanism, for one instrument, an additional spurious source, correlated with liquid water, was observed when ambient temperatures were below -5°C. These findings show that care must be taken when interpreting airborne aerosol measurements in regions of liquid water. This is particularly pertinent to studies of new particle formation by homogeneous nucleation in the vicinity of clouds.

1. Background

Airborne measurements of elevated condensation nuclei (CN) concentrations in and near marine and continental clouds have been reported by many investigators [*Radke and Hobbs*, 1969; *Saxena et al.*, 1970; *Hegg et al.*, 1990; *Hudson and Frisbie*, 1991; *Radke and Hobbs*, 1991; *Hudson*, 1993; *Perry and Hobbs*, 1994; *Clarke et al.*, 1997, 1998]. Early on, it was hypothesized that these particles were formed by splintering salt crystals during rapid drying of saline cloud droplets. Experimental studies of this mechanism, however, have been equivocal. Early studies showed evidence of salt particle splintering during crystallization [*Twomey and McMaster*, 1955; *Radke and Hegg*, 1972; *Cheng*, 1988], whereas more recent experiments did not [*Tang and Munckelwitz*, 1984; *Baumgartner et al.*, 1989; *Mitra et al.*, 1992].

Based on agreement between measurements and a physicochemical aerosol model, *Hegg et al.* [1990] concluded that layers of high CN concentrations immediately above warm marine clouds (temperatures 10° to 20°C) were formed through bimolecular nucleation of sulfuric acid and water (H_2SO_4-H_2O). They also reported measurements of high CN levels within clouds that were often congruent with cloud liquid water concentrations. The model also predicted high in-cloud CN from bimolecular H_2SO_4-H_2O nucleation, which was attributed to enhanced in-cloud actinic flux [*Hegg*, 1991].

Recent measurements in droplet-free regions of cloud venting by *Perry and Hobbs* [1994] and *Clarke et al.* [1998] support the hypothesis of new particle formation near clouds by homogeneous nucleation. Ground-based measurements have also shown evidence of new particle formation downwind of orographic clouds [*Wiedensohler et al.*, 1997]. However, airborne measurements in regions of liquid water suggest that high CN concentrations within clouds are spurious [*Hudson and Frisbie*, 1991; *Hudson*, 1993; *Clarke et al.*, 1997].

Hudson and Frisbie [1991] were among the first to attribute observations of high in-cloud CN concentrations to a sampling artifact. In warm marine stratus clouds, highest CN levels were recorded near cloud top and concentrations decreased toward cloud base. Because these observations were inconsistent with measurements near the clouds, and were only observed in clouds, Hudson and Frisbie concluded that it was a sampling artifact due to breakup of cloud droplets impacting the sampling probe. Since larger droplets would be expected to produce more fragments on impact, this mechanism could qualitatively explain the observed correlation between in-cloud CN levels and droplet size. Further measurements by *Hudson* [1993] in regions of warm marine cumulus clouds also showed enhanced CN levels, both in-cloud and below precipitating clouds. In both of these studies, aerosol was sampled through a forward facing subisokinetic inlet [*Hudson and Frisbie*, 1991; *Hudson*, 1993]. Others have also attributed airborne measurements of high CN concentrations to droplet fragmentation. During ASTEX (Atlantic

[1]Environmental Chemistry Division, Brookhaven National Laboratory, Upton, New York.
[2]School of Ocean and Earth Science and Technology, University of Hawaii, Honolulu.
[3]Research Aviation Facility, National Center for Atmospheric Research, Boulder, Colorado.
[4]Particle Technology Laboratory, Department of Mechanical Engineering, University of Minnesota, Minneapolis.

Paper number 98JD02086.
0148-0227/98/98JD-02086$09.00

Stratocumulus Transition Experiment), *Clarke et al.* [1997] observed high CN concentrations in warm clouds and below clouds in light drizzle that could only be detected by optical probe measurements [*Porter et al.*, 1992].

In this paper we study airborne measurements from the first Aerosol Characterization Experiment (ACE 1), conducted in the remote marine troposphere south of Australia (see *Bates et al.* [1998a] for ACE 1 overview), to investigate the influence of ambient conditions and aerosol sampling strategies on the generation of spurious CN by fragmenting cloud particles.

2. Breakup of Liquid Droplets

The high air speeds associated with airborne measurements, combined with the large relative size of droplets, make it likely that droplets will strike surfaces of the aerosol sampling system, such as the rim of the sampling inlet. If droplet fragments formed by impacts are aspirated with ambient aerosol particles, the measurement will be confused.

Droplet splashing is characterized by the Weber number (Wb), which relates the droplet kinetic to surface energy [e.g., *Macklin and Metaxas*, 1976] by

$$Wb = \frac{\rho R_D v^2}{\sigma} , \quad (1)$$

where ρ is the density of a droplet of radius R_D and surface tension σ, with velocity v (essentially aircraft speed). Based on the findings of *Hallett and Christensen* [1984], *Hudson and Frisbie* [1991] suggested that for Weber numbers greater than 6 (i.e., kinetic exceeds surface energy), droplets striking an inlet will fragment. This criterion is generally met for all aircraft sampling, since for a typical cloud water droplet of 10 μm radius, at standard conditions, aircraft speeds exceeding ~7 m s^{-1} (24 km h^{-1}) will satisfy the splashing criterion. In our study, the C-130 typically traveled at 100 m s^{-1}.

The number of droplet fragments aspirated is likely a complex function of many factors, such as the shape of the inlet and where, and at what angle, the droplet impacts. For example, Figure 1 shows three possible sampling scenarios. Of the three sampling conditions, most fragments are aspirated when the sample velocity at the inlet tip is greater than the aircraft speed (superisokinetic sampling), since this produces the greatest frontal area where fragments formed by impacting droplets can be swept into the inlet. Subisokinetic, or ram air, sampling could lead to few aspirated fragments since, depending on their size (inertia), fragments formed outside of the stagnation streamline may be swept out of the inlet, and droplets deflected toward the inlet inner wall would impact at shallow angles and would be less likely to disintegrate. In Figure 1, the inlets were aligned with the free stream; more extensive fragmentation is likely in misaligned inlets due to greater streamline curvature near the inlet. For this reason, flow-straightening inlet shrouds [e.g., *Torgeson and Stern*, 1966] may have a tendency to reduce the extent of droplet fragmentation.

Inlet size also influences the measured concentration of droplet fragments. Ignoring the effect of droplet size on whether a droplet strikes the inlet, and assuming the inlet is aligned with the free stream, the rate of droplet collisions with the inlet rim will be of the form

$$\Psi \cong 2\pi R \cdot t \cdot N_c \cdot v , \quad (2)$$

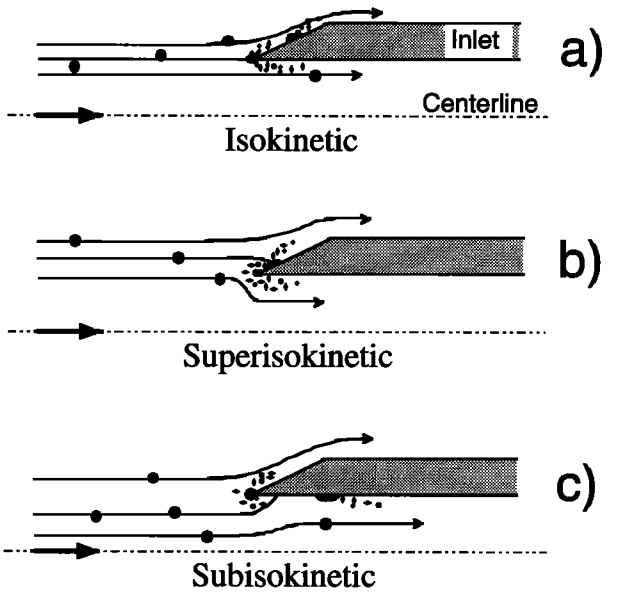

Figure 1. Cartoon showing generation of droplet fragments by droplets striking an airborne aerosol inlet. Three sampling situations are shown: (a) isokinetic, (b) anisokinetic sampling where the sample velocity is higher than the free stream, (c) anisokinetic (ram air sampling) in which the sample velocity is lower than the free stream velocity. Different sampling scenarios will affect the number of fragments aspirated.

where the rate of collisions (Ψ) is the cross-sectional area where droplets impact and the resulting fragments are aspirated, times the product of the droplet concentration (N_C) and the aircraft speed (v). We have assumed that the thickness (t) of the annular-shaped area of impaction around the inlet rim where fragments are aspirated is much smaller than R. Depending on the sampling conditions, this may not always be true. Assuming the aerosol is well mixed in the sampling lines by the time it is detected, the number concentration of detected droplet fragments (Nf) will be,

$$N_f = (fragments / collision)\left(\frac{collisions / time}{volume\ sampled / time}\right) = X\frac{\Psi}{Q} \cong \frac{2 X N_c t}{R} , \quad (3)$$

where X is the number of fragments formed per droplet impact, and Q is the volumetric sample flow rate. For isokinetic sampling, Q equals the aircraft speed times the cross-sectional area of the inlet (πR^2). Combining this with (2), we obtain the right-hand term in (3).

The number of fragments formed per collision (X) considers only those impacts which lead to aspirated fragments. X depends on many factors, one of which is likely the droplet volume concentration (liquid water concentration). Note that (3) predicts that the concentration of droplet fragments depends on inlet size, so smaller inlets (smaller R) should produce higher concentrations of droplet fragments. This is due to scaling, since smaller inlets have higher perimeter to cross-sectional area ratios than do larger ones, leading to higher fragment concentrations, if the fragments are formed primarily along the inlet perimeter.

3. ACE 1 Airborne Aerosol Inlets and Instrumentation

Two different aerosol inlets were deployed on the National Center for Atmospheric Research (NCAR) C-130 research aircraft for the ACE 1 campaign (see, for example, *Bates et al.* [1998a]). Practically all condensation particle counters (CPCs) on the aircraft sampled from the community aerosol inlet (CAI). Mounted on the side, the tip of the CAI extended to near the front of the aircraft. The inlet was actively controlled to maintain isokinetic sample flow rates. The tip of the CAI is shown in Figure 2a. The inlet was shrouded and the tip was blunt with a 0.13 cm radius and inside diameter of ~4 cm. The CAI was unusually long, with an overall length of 6.74 m, and was composed of a series of three diffuser sections, each followed by a straight section. The flow was slowed by a factor of 10 by the time it reached the extraction plane, where various instruments sampled isokinetically via individual sampling tubes ranging in diameter from 0.625 to 1 inch (1.59 to 2.54 cm). These individual sampling tubes immediately made a sweeping 90° bend to enter perpendicular to the aircraft wall. With a Reynolds number at standard conditions of ~10^5, the flow throughout the CAI was turbulent and the aerosol well mixed at the sampling plane.

The other aerosol inlet was located on the aircraft belly about halfway aft and situated roughly 21 cm from the aircraft skin.

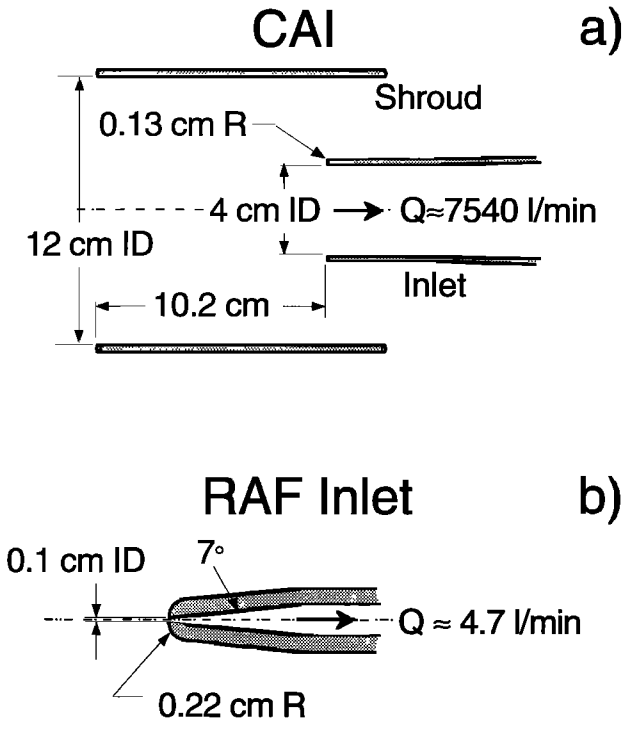

Figure 2. Size comparison of two airborne aerosol inlets, (a) CAI and (b) RAF, deployed on the NCAR C-130 during ACE 1. The drawings are not to scale, and the scales for Figures 2a and 2b differ. Only the tip of the community aerosol inlet (CAI) is shown, the complete inlet was ~6.7 m long. The CAI served as a common inlet for a variety of instruments and is much larger than the RAF inlet which sampled for a single instrument. l/min denotes liters per minute.

This inlet was nominally isokinetic, but the flow rate was not actively controlled to maintain isokinetic sampling. Shown in Figure 2b, the inlet was much smaller than the CAI with a tip inside diameter of ~0.1 cm. From the tip, the inlet expanded at roughly a 7° angle to 1.02 cm, the inside diameter of a 1.27 cm (0.5 inch) sampling tube which ran to a single TSI 3760 CPC (TSI Inc., St. Paul, Minnesota). We refer to this inlet and CPC as the RAF inlet (NCAR Research Aviation Facility) and RAFCPC.

A summary of the various aerosol instrumentation discussed in this paper is given in Table 1. To aid comparison of aerosol concentrations measured at different altitudes, all CN concentrations are reported at standard temperature and pressure (20°C, 1 atm). In addition to the instruments within the aircraft, aerosol optical probes were mounted on the wings. We use the FSSP100 (forward scattering spectrometer probe) to derive cloud water and ice content. In liquid water clouds, the FSSP probe provides a good estimate of cloud water content; however, due to errors in sizing ice particles, in mixed clouds, FSSP-derived cloud water and ice content can be in significant error, depending on the size and shape of the ice particles [*Gardiner and Hallett*, 1985; *Gayet et al.*, 1996]. Liquid water was also measured with a hot wire PMS King Probe (Particle Measuring Systems, Boulder, Colorado), but because the absolute value of this measurement drifted with temperature, the FSSP-derived liquid water content was generally used instead.

4. Results and Discussion

4.1. Observations of High CN Levels in Warm Regions With Liquid Water

4.1.1. Correlation with liquid water. Many episodes of unusually high particle concentrations were observed in and around clouds during the ACE 1 campaign. Because it was known that sampling in regions of liquid water could result in spurious measurements, and the instrumentation and inlets were not designed for this type of sampling, regions containing liquid water were usually avoided. However, during ferrying flights and Lagrangian studies in which the aircraft attempted to continually sample from one air parcel, the position of the aircraft was restricted and sampling in-cloud and in precipitation was often unavoidable.

In the first ACE 1 Lagrangian study (see, for example, *Suhre et al.*, [1998]) most of the flight was spent in the boundary layer which extended up to ~1300 m above sea level and contained layers of broken stratocumulus and scattered cumulus clouds. This resulted in many brief episodes of in-cloud sampling. At boundary layer temperatures between 2.6° and 11.6°C, the clouds were liquid water. Figure 3 shows FSSP-measured liquid water concentration and altitude during this Lagrangian study. Focusing on the measurements within the boundary layer (altitude less than 1300 m in Figure 3), measurements when FSSP liquid water concentrations were greater than 0.01 g kg^{-1} are shown by solid circles. The value of 0.01 g kg^{-1} was arbitrarily chosen as the cutoff for the presence of water droplets. The corresponding CN concentrations are shown in Figure 4, and particle concentrations when FSSP liquid water levels were greater than 0.01 g kg^{-1} are again identified by solid circles. Figure 4 shows that periods of high particle concentrations were observed in regions of liquid water. Note that in Figure 4a, in-cloud RAF CN_{15} (CN larger than 15 nm diameter)

Table 1. ACE 1 Airborne Aerosol Inlets and Instrumentation

	Instrument	Measurement Acronym	Measurement Size Range	Comment
CAI				
	TSI 3025	CN_3	$D_p > 3$ nm	
	TSI 3010	CN_{10}	$D_p > 10$ nm	
	TSI 3760	RCN_{15}	$D_p > 15$ nm	inlet heated to 300°C
	PHA UCPC	PHA CN_3	$D_p > 3$ nm	
	PHA UCPC	nanoparticles (estimate only)	nominally $3 < D_p < 4$ nm	
RAF inlet				
	TSI 3760	RAF CN_{15}	$D_p > 15$ nm	
Wing-mounted optical probe				
	FSSP100		$2 < Dp < 47$ μm	derived cloud water + ice content

TSI denotes Thermo Systems, Inc., St. Paul, Minnesota. CN denotes condensation nuclei. RCN denotes refractory condensation nuclei. PHA UCPC denotes pulse height analysis ultrafine condensation particle counter. Dp stands for particle diameter. FSSP100 is Particle Measuring Systems (PMS, Boulder, Colorado) forward scattering spectrometer probe.

concentrations are orders of magnitude higher than clear air levels (no solid circles). Figures 4b and 4c show aerosol concentrations measured from the CAI; Figure 4b shows the concentrations of PHA CN_3 (CPC with pulse weight analysis measuring CN larger than 3 nm diameter), and Figure 4c shows an estimate of the nanoparticle concentration (particles with diameters nominally between 3 and 4 nm, (see *Weber et al.* [1995] for a description of the measurement). Compared to the magnitude of RAF CN_{15} in Figure 4a, in Figure 4b the maximum concentrations of PHA CN_3, during periods of high liquid water, were about an order of magnitude lower. This appears to be from inlet differences, since all CPCs sampling from the CAI recorded similar levels during these episodes.

Figure 4c shows that nanoparticles were also correlated with liquid water, suggesting that the mechanism causing high CN also produced particles as small as 3 to 4 nm diameter. The observation of nano-sized particles in regions of liquid water was not unique to the PHA UCPC (ultrafine condensation particle counter). The difference in CN_3 and CN_{10} (TSI 3025 UCPC and a TSI 3010 CPC) at these times also indicated the presence of significant numbers of in-cloud particles between ~3 and 10 nm diameter. However, compared to the total numbers recorded in-cloud, nanoparticles made up only a small fraction and thus differences in CPC lower detection limits (shown in Table 1) will have little influence when comparing total CN concentrations from the various instruments.

The particle concentrations recorded during periods of high liquid water are not consistent with clear air measurements; however, the clear air measurements between the liquid water (cloud) penetrations are consistent with the findings of other researchers. Typical remote marine boundary layer CN levels range from 200 to 500 cm^{-3} [*Hoppel and Frick*, 1990; *Fitzgerald*, 1991; *Covert et al.*, 1996; *Bates et al.*, 1998b]. For the episode shown in Figure 3 when FSSP liquid water was less than 0.01 g kg^{-1}, the median aerosol concentrations recorded by all CPCs sampling from the CAI and the RAF inlet were similar, ~ 400 cm^{-3}, typical of background levels. However, when liquid water was present, the RAF CN_{15} values were 2 orders of magnitude higher than background levels, whereas the concentrations recorded by various CPCs from the CAI were about 1 order of magnitude higher. Other researches, who attributed high in-cloud CN to droplet fragmentation, report levels of

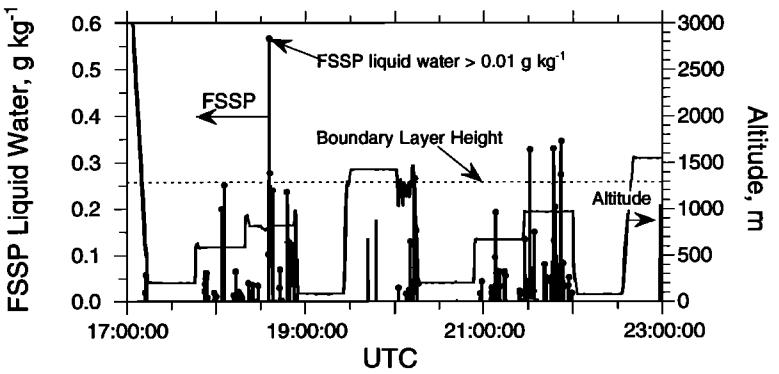

Figure 3. FSSP-derived cloud liquid water concentrations measured during an ACE 1 Lagrangian study (flight 18, December 1, 1995). Spikes in water concentrations are periods of cloud penetrations. Solid circles identify episodes when sampling in the boundary layer (altitude less than 1300 m) and when FSSP liquid water concentrations exceeded 0.01 g kg^{-1}. During these periods, temperatures ranged between ~3° and 12°C.

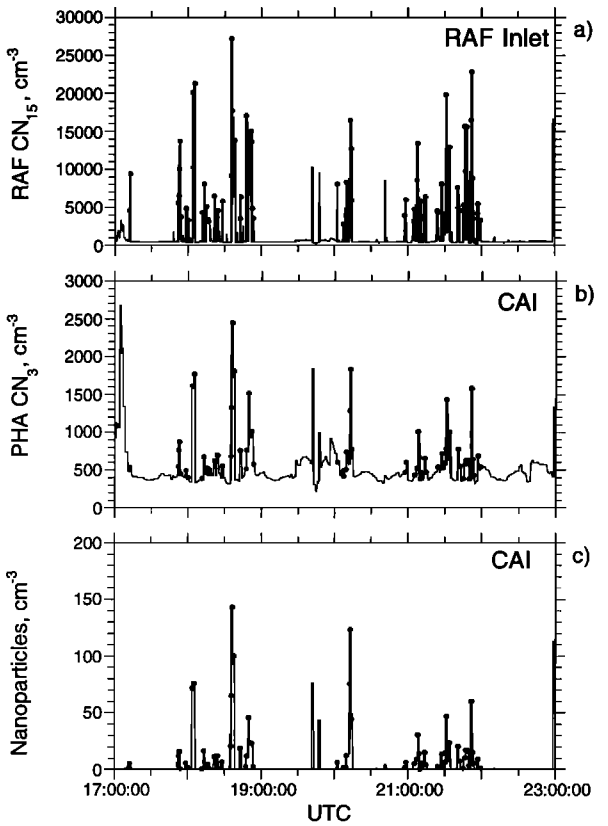

Figure 4. Particle concentrations for the period shown in Figure 3. Solid circles indicate the presence of liquid drops. Spikes in both particle and nanoparticle concentrations were observed in regions of liquid water. The size of particles detected for the various CPCs plotted is shown in Table 1. The figure shows that highest particle concentrations were recorded by the RAF CPC sampling from the RAF inlet in regions of liquid water.

in-cloud CN of the order of 10^3 cm^{-3} [*Hudson and Frisbie*, 1991; *Hudson*, 1993; *Clarke et al.*, 1997], similar to our measurements from the CAI. The in-cloud CN concentrations observed by *Hegg* [1991], which were attributed to in-cloud nucleation, were lower, ranging from 500 to 600 cm^{-3}.

If these abnormal CN levels were from fragmenting droplets, their concentrations should be correlated with liquid water concentrations. Figure 5 shows the RAF CN_{15} and PHA CN_3 concentrations with respect to liquid water, for the measurements identified by solid circles in Figure 3. The RAF CN_{15} were highly correlated with FSSP liquid water ($r = 0.92$), while the PHA CN_3 were not as well correlated ($r = 0.53$). RAF CN_{15} concentrations in-cloud were also correlated with the cloud droplet number concentration and cloud droplet diameter ($r=0.80$ and 0.85, respectively).

The correlation between aberrant CN levels and liquid water suggests that the source of these particles was shattering of water droplets. To further explore this hypothesis we compare CN and refractory CN concentrations to test if the observations are consistent with droplet disintegration.

4.1.2. Sources of high CN concentrations in the vicinity of clouds. Three mechanisms have been proposed as potential sources of particles within and near clouds: (1) splintering of rapidly drying sea-salt crystals, (2) homogeneous nucleation, and (3) spurious measurements from droplets fragmenting upon impact with sampling surfaces. The measurement of refractory CN (RCN; particles that remain after heating to 300°C) can help delineate these mechanisms of particle formation. For example, in remote marine regions, refractory material can be sea salt, crustal material, or soot, whereas freshly formed particles are likely sulfuric acid or ammonium (bi)sulfate, both of which volatilize at temperatures below 300°C [*Clarke*, 1991]. *Clarke et al.* [1997] showed from ASTEX measurements that in regions of liquid water, both CN and RCN_{15} were correlated with liquid water concentrations. Since homogeneous nucleation produces particles that are not refractory, and splintering of drying salt crystals would not likely be correlated with liquid water, their data suggested that the particles were formed by shattering droplets that contained dissolved refractory material, such as sea salt. Here we do a similar analysis using measurements of CN_{10} and RCN_{15} from the CAI to contrast the measurements of high CN recorded within clouds to the high CN levels measured in regions of cloud venting.

Focusing first on CN measurements in regions of liquid water, for the abnormally high in-cloud particle levels of Figures 3 and 4, Figure 6a shows that these particles were highly correlated with RCN_{15}, and thus many of them were composed of refractory material. This is consistent with particle formation by breakup of cloud droplets containing dissolved sea salt. An interesting feature of Figure 6a is that the slope of the curve is ~1.5, significantly higher than 1. We do not believe that CPC sample flow rate uncertainties, or differences in CPC lower size detection limit (see Table 1) can account for all of this system-

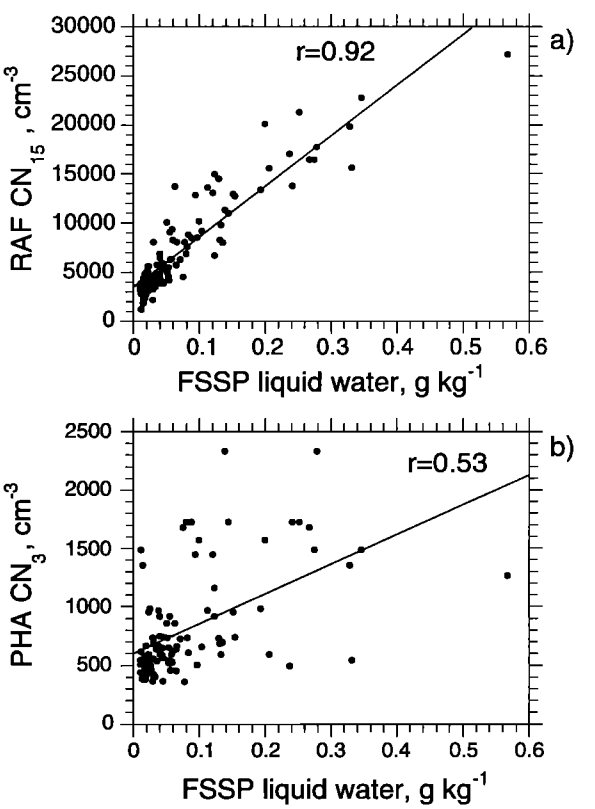

Figure 5. Correlation of CN measured from (a) the RAF inlet and (b) the CAI with FSSP liquid water for the episodes identified by solid circles in Figures 3 and 4. These are periods when FSSP liquid water concentrations were greater than 0.01 g kg^{-1}.

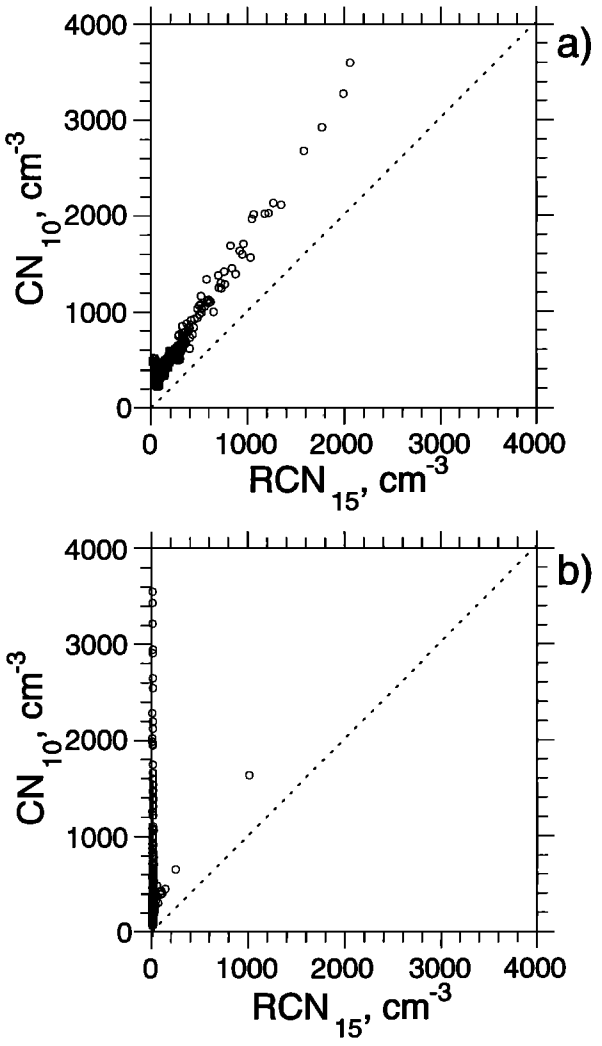

Figure 6. Comparison of CN_{10} to RCN_{15} (refractory CN, aerosols which survive heating to 300°C) (a) for the boundary layer measurements shown in Figures 3 and 4 when high particle concentrations were correlated with liquid water (flight 18, December 1, 1995), and (b) during studies in the vicinity of clouds when liquid water levels were less than 0.01 g kg^{-1} (flight 27, December 10, 1995). Figure 6a shows that many of the particles observed in-cloud were composed of refractory material, consistent with the hypothesis that they were spurious fragments from shattering water droplets containing sea salt. Figure 6b shows that particles recorded near clouds in regions of no liquid water were volatile, consistent with expectations that these particles were authentic, resulting from nucleation of gas species.

atic concentration difference. The difference may in part be due to the cloud droplets being an external mixture of salt and a nonrefractory material, such as non-sea-salt sulfate.

In contrast to the in-cloud CN of Figure 6a, Figure 6b shows CN_{10} versus RCN_{15} in regions of cloud venting where high particle concentrations have been observed and attributed to homogeneous nucleation [*Clarke et al.*, 1998]. The measurements in Figure 6b are from flight 27 in regions near clouds, but where FSSP water concentrations were less than 0.01 g kg^{-1}. This flight was aimed at studying new particle formation in clear air regions of cloud venting. Unlike the measurements in regions containing liquid water, practically all of these particles were volatile, and were likely formed by homogeneous nucleation. The particles were not splintered sea-salt crystals, since this would produce refractory CN. Note that based on the magnitude of the CN_{10} concentrations, the spurious droplet shatter measurements in Figure 6a and the authentic measurements of Figure 6b are very similar. Thus based only on measured CN concentrations, there is no clue that in one case the measurements are a sampling artifact and in the other the measurements are real. This analysis emphasizes the utility of the refractory CN measurement when studying new particle formation in the vicinity of marine clouds.

4.1.3. Influence of inlet geometry on fragment concentrations. Our analysis shows that fragmentation of liquid water led to spurious particle measurements. However, similar measurement techniques from two different inlets on the same aircraft produced large discrepancies in particle concentrations. Figure 4 showed that in-cloud particle concentrations were much higher for the RAF inlet compared to those recorded from the CAI. This was consistently observed in regions of liquid water throughout the ACE 1 study. For example, Figure 7a compares

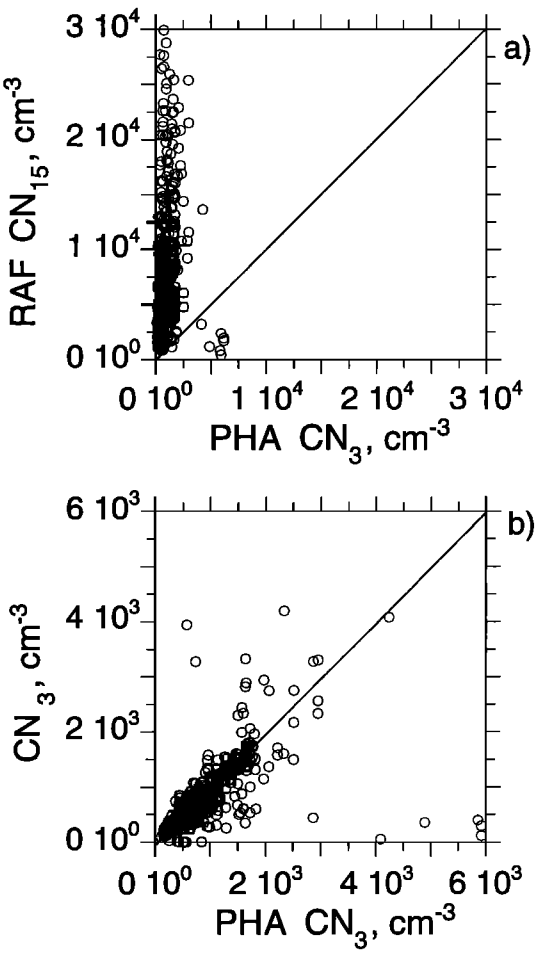

Figure 7. Comparison of elevated CN levels due to droplet fragmentation (a) from the RAF inlet and CAI and (b) from two UCPCs both sampling from the CAI. Plots show all episodes during ACE 1 (30 flights) when FSSP liquid water concentrations were larger than 0.01 g kg^{-1} and temperatures greater than 0°C. The RAF inlet produced much higher fragment concentrations.

measurements from the two inlets, RAF CN_{15} to PHA CN_3, for all ACE 1 data (all flights) when FSSP water levels were greater than 0.01 g kg^{-1}, and when temperatures were greater than 0°C. Although the fragment concentrations between the two inlets differed greatly, for these conditions, CN levels were similar for the CPCs sampling from the CAI; Figure 7b compares CN_3 to PHA CN_3. For the data shown, the ratio of RAF CN_{15} to PHA CN_3 had a mean value and standard deviation of 11±9, and the ratio of CN_3 to PHA CN_3 was 0.95±0.5. Thus in regions of liquid water, CN measurements from the RAF inlet were typically an order of magnitude higher than those from the CAI.

To compare fragmentation from the two inlets, we use (3) to predict the ratio of fragment number concentrations in the RAF inlet to CAI. Considering only differences in inlet size, (i.e., assuming equal X, t, and N_C in (3)), the ratio is approximately

$$\frac{N_{f(RAF)}}{N_{f(CAI)}} \cong \frac{R_{CAI}}{R_{RAF}} = \frac{20}{0.5} = 40 \ , \qquad (4)$$

where R_{CAI} and R_{RAF} are the inside radii of the CAI and RAF inlet, respectively (see Figure 2). This suggests that in terms of droplet fragmentation, the two inlets behaved similarly, and observed differences in spurious CN concentrations were primarily due to differences in inlet size.

4.2. Observations of High Particle Concentrations in Cold Regions of Liquid Water

4.2.1. Comparison of fragmentation in warm and cold regions. Abnormally high particle concentrations were also observed in higher altitude clouds where temperatures were considerably below 0°C; however, there were significant differences from the episodes of warm droplet fragmentation discussed above. Excluding PHA CN_3 concentrations for the moment, particle concentrations were lower in cold clouds. For example, in cold clouds, maximum RAF CN_{15} concentrations were of the order of 10^3 cm^{-3}, still high above background levels of ~10^2 cm^{-3}, but about an order of magnitude lower than in warm clouds. Both the UCPC and CPC, sampling from the CAI, generally did not show significant evidence of shatter during these periods. This is fairly consistent with the RAF CN_{15} measurements, since a factor of ~40 lower fragment concentration than RAF levels, due to inlet size, puts CAI CN concentrations near background levels.

A notable exception to these observations was the concentration of PHA CN_3. In cold clouds, PHA CN_3 concentrations did not agree with the other CAI CN measurements and were even much higher than RAF CN_{15} levels. The source of anomalous PHA CN_3 in cold clouds is discussed in a following section.

To compare fragmentation of cloud particles in cold and warm clouds, we focus on the RAF CN_{15} measurements. Figure 8a compares RAF CN_{15} levels versus FSSP cloud water plus ice content for warm and cold clouds. This plot includes the warm in-cloud measurements of Figure 4 and additional warm and cold in-cloud measurements from other flights. The warm in-cloud measurements were made at altitudes of 0.5 to 1 km above sea level, whereas the cold measurements were at altitudes ranging from about 5 to 6 km above sea level. In the cold clouds, at temperatures near -20°C, most water is likely to be in the ice phase, with the possibility of some supercooled droplets [*Moss and Johnson*, 1994]. Figure 8a shows that just as in the warm cloud cases, CN recorded in cold clouds were also

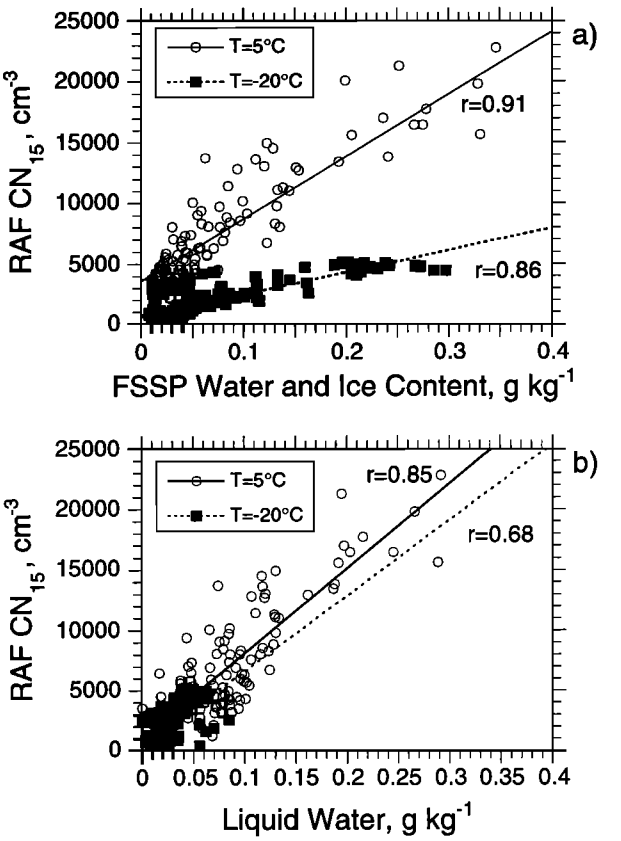

Figure 8. (a) Comparison of RAF CN_{15} concentrations versus FSSP water plus ice concentrations for warm and cold conditions. Two separate measurement episodes are shown for each case. The average temperature and standard deviation for the two warm events were 5±1°C and 4±2°C, and for the cold events, -20±1°C and -19±1°C. The number of fragments (essentially the CN concentration) is considerably lower for the colder conditions at similar FSSP water and ice concentrations. (b) The same data plotted as a function of liquid water concentration (hot wire measurement) showing that fragmentation was similar when only liquid water is considered. The liquid water measurements were translated so that no measurements were below zero to account for a temperature dependent offset in the liquid water measurement.

correlated with cloud FSSP water plus ice concentration. In this case the FSSP cloud water and ice content is only an estimate due to limitations in inferring ice particle sizes from light scattering. In any case, the liquid water content of these cold clouds would be significantly less than in the warm clouds. If only liquid water droplets fragment, then CN concentrations from fragmenting droplets should be much higher in warm clouds, as shown in Figure 8a. Considering only the cloud liquid water content, Figure 8b shows that liquid drops in warm and cold clouds fragment in a similar manner.

This analysis suggests that ice particles generally did not fragment, or fragmented to a much lesser extent than liquid drops. This was also observed in other flights when ambient temperatures were below -25°C and FSSP water plus ice concentrations were greater than 0.01 g kg^{-1}. At these times, the average RAF CN_{15}, PHA CN_3, and CN_3 ranged from 250 to 270 cm^{-3}, concentrations typical for these remote regions. However, even at these low temperatures, there were a few brief

events where concentrations exceeded ~10^3 cm^{-3}, indicative of fragmenting droplets. Thus even in very cold regions, evidence for droplet shatter can occasionally be observed.

4.2.2. Aberrant PHA CN_3 concentrations in cold regions. Periods when PHA CN_3 levels were higher than all other CPCs during in-cloud measurements were recorded throughout the ACE 1 study, but were only observed over a limited temperature range. Figure 9 compares PHA CN_3 and CN_3 levels by plotting the ratio of the two measurements when temperatures were between +20° and -40°C and FSSP water and ice content was greater than 0.01 g kg^{-1}. For clarity, the median of the ratio of data binned by temperature is plotted as a line. Figure 9 shows that PHA CN_3 levels were generally significantly higher than CN_3 levels when temperatures ranged between approximately -5° and -25°C. At higher temperatures, concentrations of fragmenting drops were similar for the PHA CN_3 and CN_3, as shown previously in Figure 7b.

These episodes were also correlated with FSSP cloud water-ice content. For the -20°C data of Figure 8, the correlation coefficient between PHA CN_3 and FSSP water and ice was 0.70, and the correlation with liquid water was 0.57. Since these episodes are found primarily in regions of supercooled water (-5° to -25°C), it suggests that droplet fragmentation played a role, but the cause is unknown. Tests during these episodes showed that these results were unique to the PHA UCPC sampling line and not due to the PHA UCPC instrument itself. A crossover sample line installed between the PHA UCPC and UCPC, at the entrance to each instrument, allowed both instruments to sample from the same line. During these cold in-cloud episodes, both CPCs recorded "low" (near background) particle concentrations when sampling from the UCPC line and extremely high levels when sampling from the PHA UCPC line.

These observations limit explanations to either differences in locations on the sampling plane within the CAI where individual CPCs extract a sample, or differences in the aerosol transport tubing running from the CAI to individual CPCs. Sample line differences are the likely cause since the aerosol in the CAI was well mixed (Reynolds number ~10^5) and the PHA UCPC did

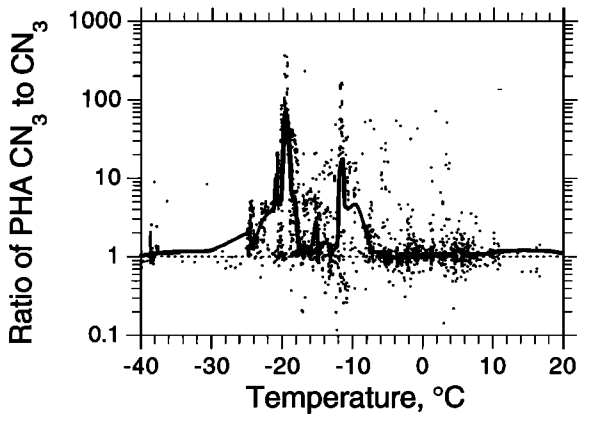

Figure 9. Ratio of PHA CN_3 to CN_3 as a function of temperature during measurements when droplet fragmentation could occur (FSSP water plus ice concentrations greater than 0.01 g kg^{-1}). The line is the median of the ratio. For temperatures higher than approximately -5°C the two measurements generally agreed, as shown in Figure 7b. However, at temperatures below -5°C, PHA CN_3 levels could be orders of magnitude higher. The cause is unknown but thought to be related to droplet fragmentation, possibly within the aerosol sampling line.

employ a unique aerosol plumbing system. In this system, in order to minimize 3-10 nm particle transport losses, a portion of the sample flow was extracted from the centerline of the tube by a smaller thin-walled tube. There were two centerline samplers within the PHA UCPC sampling line. The first split the flow immediately after it entered the cabin, and the second was located approximately 5 m further down the sampling line, just prior to sampling by the PHA UCPC. Both were nominally isokinetic.

One explanation for these spurious measurements is droplet fragmentation at these centerline extraction points. The high correlation of these events with liquid water suggests fragmentation played a role; however, observations show that fragmentation could only occur in the sampling line when temperatures were between roughly -5° and -25°C. Moreover, it is unlikely that the large cloud droplets or ice particles penetrated far into our sampling lines.

Another possibility is formation of particles within the sample line by nucleation, possibly involving water vapor. A supersaturated vapor could be created by depressing the temperature at a constriction in the sampling line. Drying fragments could also be a source of water vapor. Based on our measurements and sampling system, neither appears to be a viable explanation. Again, it is unclear why this mechanism was favored at cold temperatures.

Although we have no thorough explanation for why PHA CN_3 levels were much higher than all other CPCs in cold regions containing cloud water, it appears to be related to fragmentation of cloud droplets and our use of centerline sampling within the aerosol transport tubing.

4.3. Approaches for Minimizing Droplet Fragmentation

Because fragmentation precludes accurate measurements of ambient aerosols in regions with liquid water, sampling techniques to eliminate droplet shatter are needed. This could be done by situating the inlet in a region where droplets are excluded or by designing an inlet to remove fragments. To exclude cloud droplets in studies of particle formation near clouds, *Perry and Hobbs* [1994] placed their inlet close to the aircraft skin (1.25 cm) when sampling in-cloud. It is unclear how effective this technique was since their measurements were made at high altitudes in cold regions (less than -20°C) where, based on our studies, fragmentation would be unlikely. Another approach is to point the inlet backward [e.g., *Schröder and Ström*, 1997]. Cloud droplets would impact the back of the inlet, and only fragments small enough to negotiate the 180° bend to enter the inlet would be aspirated. This may exclude most fragments, yet our data suggest that fragments can reach sizes as small as a few nanometers in diameter which would not be excluded with this type of sampling.

Sharp tip inlets sampling isokinetically would minimize fragmentation by presenting the least frontal surface area for droplet impaction. However, these inlets are prone to flow separation near the tip, which can result in enhanced particle losses in the separation region. Ram air sampling may improve the situation by tending to exclude droplet fragments formed near the perimeter of the inlet tip, since the flow in this region reverses and does not enter the inlet.

Recent work on a low-turbulence inlet [*Seebaugh and Lafleur*, 1996], designed to reduce inlet particle losses through turbulent deposition, may also remove droplet fragments. In this inlet, porous walls remove the turbulent boundary layer along

the inlet walls. Since most fragments are formed near the tip along the perimeter, this suction could also remove droplet fragments.

Finally, if fragmentation of droplets cannot be completely eliminated, it may be more desirable to have a sampling system that produces large numbers of spurious CN, making their presence obvious, versus a system which produces spurious concentrations at levels similar to ambient aerosol concentrations. For example, because the RAFCPC recorded exceptionally high particle concentrations in regions of liquid water during ACE 1, these measurements could be used as a marker for identifying periods when all aerosol measurements were suspect.

5. Conclusions

Airborne measurements of aerosols within and in the vicinity of clouds can be confused by spurious particles formed by liquid droplets fragmenting on impact with sampling surfaces. Measurements from ACE 1 showed that concentrations of droplet fragments were correlated with liquid water levels for both warm and supercooled droplets (temperatures as low as -20°C). Ice particles, however, generally did not appear to fragment. Concentrations of droplet fragments also depended on inlet size. Inlets with smaller openings can produce higher fragment concentrations because of higher perimeter to cross-sectional area ratios, since fragment-forming impacts are most likely along the perimeter of the inlet, and the sample volume depends on the cross-sectional area for an isokinetic inlet.

Not all of the observations of fragmentation could be explained. Measurements showed that particles down to 3 nm diameter were produced by fragmenting droplets. It is unclear how 3 to 4 nm diameter particles could be generated by mechanical means since mechanical breakup of liquids typically results in droplets of the order of 1 μm diameter. Though fragments drying in the aerosol sample line will shrink, it seems unlikely this will lead to large reductions in particle size (i.e., maximum diameter changes of factors of ~2 would be expected for sulfuric acid and ammonium (bi)sulfate particles [*Nemesure et al.*, 1995]). We also observed spurious CN in an aerosol sampling system designed to minimize particle losses by extracting sample aerosol from the centerline of the tube. The source of these spurious CN is unknown, but it appears that a combination of cloud particle fragmentation and the obstruction presented by the centerline sampler led to the generation of large numbers of particles within the aerosol sampling line. This was only observed when temperatures ranged between roughly -5° and -25°C.

The possibility that spurious CN can be generated in regions of liquid water, such as within and near clouds, may have influenced past interpretations of new particle formation in the remote troposphere. Based on airborne CN measurements, bimolecular (H_2SO_4-H_2O) homogeneous nucleation has been proposed both within [*Hegg*, 1991] and in the vicinity of marine clouds [*Hegg et al.*, 1990; *Perry and Hobbs*, 1994; *Clarke et al.*, 1998]. We also observed high CN concentrations in these regions. However, our in-cloud CN were a different composition than particles observed in regions of cloud venting. We have shown that our in-cloud CN were spurious since they were correlated with liquid water concentrations and were often composed of refractory material (CN that survive heating to 300°C), precluding the possibility that they were formed by homogeneous nucleation. In contrast, CN sampled in clear air adjacent to clouds appeared to be authentic since they were volatile at 300°C, consistent with particles recently formed by homogeneous nucleation. This analysis shows that care must be taken when interpreting measurements of aerosols in regions containing liquid water, particularly studies of new particle formation near clouds.

Acknowledgments. The authors thank Cynthia Twohy for her insightful comments and Darrel Baumgardner for use of his optical probe data. Research at BNL was performed under the auspices of the U.S. Department of Energy contract DE-AC02-98CH10886 Atmospheric Chemistry Program within the Office of Health and Environmental Research. Additional support included U.S. Department of Energy grant DE-FG02-91ER61205. This research is a contribution to the International Global Atmospheric Chemistry (IGAC) Core Project of the International Geosphere-Biosphere Program (IGBP) and is part of the IGAC Aerosol Characterization Experiments (ACE).

References

Bates, T. S., B. J. Huebert, J. L. Gras, F. B. Griffiths, and P. A. Durkee, The International Global Atmospheric Chemistry (IGAC) Project's First Aerosol Characterization Experiment (ACE1); Overview, *J. Geophys Res., 103*, 16297-16318, 1998a.

Bates, T. S., V. N. Kapustin, P. K. Quinn, D. S. Covert, D. J. Coffman, C. Mari, P. A. Durkee, W. J. De Bruyn, and E. S. Saltzman, Processes controlling the distribution of aerosol particles in the lower marine boundary layer during the First Aerosol Characterization Experiment (ACE1), *J. Geophys. Res., 103*, 16369-16383, 1998b.

Baumgartner, F., A. Zanier, and K. Krebs, On the mechanical stability of hollow NaCl particles, *J. Aerosol Sci., 20*, 883-886, 1989.

Cheng, R., The generation of secondary marine aerosols, *Lect. Notes Phys., 298*, 589-592, 1988

Clarke, A. D., A thermo-optic technique for in situ analysis of size resolved aerosol physicochemistry, *Atmos Environ., 25A*, 635-644, 1991.

Clarke, A. D., T. Uehara, and J. N. Porter, Atmospheric nuclei and related aerosol fields over the Atlantic: Clean subsiding air and continental pollution during ASTEX, *J. Geophys. Res., 102*, 25281-25292, 1997.

Clarke, A. D., J. L. Varner, F. Eisele, R. L. Mauldin, D. Tanner, and M. Litchy, Particle production in the remote marine atmosphere: Cloud outflow and subsidence during ACE1, *J. Geophys. Res., 103*, 16397-16409, 1998.

Covert, D. S., V. N. Kapustin, T. S. Bates, and P. K. Quinn, Physical properties of marine boundary layer aerosol particles of the mid-Pacific in relation to sources and meteorological transport, *J. Geophys. Res., 101*, 6919-6930, 1996.

Fitzgerald, J. W., Marine aerosols: A review, *Atmos. Environ., 25A*, 533-545, 1991.

Gardiner, B. A., and J. Hallett, Degradation of in-cloud forward scattering spectrometer probe measurements in the presence of ice particles, *J. Atmos. Oceanic Technol., 2*, 171-180, 1985.

Gayet, J. F., G. Febvre, and H. Larsen, The reliability of the PMS FSSP in the presence of small ice crystals, *J. Atmos. Oceanic Technol., 13*, 1300-1310, 1996.

Hallett, J., and L. Christensen, Splash and penetration of drops in water, *J. Rech. Atmos., 18*, 226-242, 1984.

Hegg, D. A., Particle production in clouds, *Geophys. Res. Lett., 18*, 995-998, 1991.

Hegg, D. A., L. F. Radke, and P. V. Hobbs, Particle production associated with marine clouds, *J. Geophys. Res., 95*, 13917-13926, 1990.

Hoppel, W. A., and G. M. Frick, Submicron aerosol size distributions measured over the tropical and South Pacific, *Atmos. Environ., 24A*, 645-659, 1990.

Hudson, J. G., Cloud condensation nuclei near marine cumulus, *J. Geophys. Res., 98*, 2693-2702, 1993.

Hudson, J. G., and P. R. Frisbie, Cloud condensation nuclei near marine stratus, *J. Geophys. Res., 96*, 20795-20808, 1991.

Macklin, W. C., and G. J. Metaxas, Splashing of drops on liquid layers, *J. Applied Phys., 47*, 3963-3970, 1976.

Mitra, S. K., J. Brinkmann, and H. R. Pruppacher, A wind tunnel study on the drop-to-particle conversion, *J. Aerosol Sci., 23*, 245-256, 1992.

Moss, S. J., and D. W. Johnson, Aircraft measurements to validate and improve numerical model parametrizations of ice to water ratios in clouds, *Atmos. Res., 34*, 1-25, 1994.

Nemesure, S., R. Wagener, and S. E. Schwartz, Direct shortwave forcing of climate by the anthropogenic sulfate aerosol: Sensitivity to particle size, composition, and relative humidity, *J. Geophys. Res., 100*, 26105-26116, 1995.

Perry, K. D., and P. V. Hobbs, Further evidence for particle nucleation in clear air adjacent to marine cumulus clouds, *J. Geophys. Res., 99*, 22803-22818, 1994.

Porter, J. N., A. D. Clarke, G. Ferry, and R. F. Pueschel, Aircraft studies of size-dependent aerosol sampling through inlets, *J. Geophys. Res., 97*, 3815-3824, 1992.

Radke, L. F., and D. A. Hegg, The shattering of saline droplets upon crystallization, *J. Rech. Atmos., 6*, 447-455, 1972.

Radke, L. F., and P. V. Hobbs, Measurements of cloud condensation nuclei, light scattering coefficient, sodium-containing particles, and Aitken nuclei in the Olympic Mountains of Washington, *J. Atmos. Sci., 26*, 281-288, 1969.

Radke, L. F., and P. V. Hobbs, Humidity and particle fields around some small cumulus clouds, *J. Atmos. Sci., 48*, 1190-1193, 1991.

Saxena, V. K., J. N. Burford, and J. L. Kassner Jr., Operation of a thermal diffusion chamber for measurements on cloud condensation nuclei, *J. Atmos. Sci., 27*, 73-80, 1970.

Schröder, F., and J. Ström, Aircraft measurements of sub micrometer aerosol particles (>7nm) in the midlatitude free troposphere and tropopause region, *Atmos. Res.*, 44, 333-356, 1997.

Seebaugh, W. R., and B. G. Lafleur, Low turbulence inlet for aerosol sampling from aircraft, paper presented at American Association for Aerosol Research, Orlando Fla., Oct. 14-18, 1996.

Suhre, K., et al., Physico-chemical modeling of the First Aerosol Characterization Experiment (ACE1) Lagrangian B., 1., A moving column approach., *J. Geophys. Res., 103*, 16433-16455, 1998.

Tang, I. N., and H. R. Munckelwitz, An investigation of solute nucleation in levitated solution drops, *J. Colloid Interface Sci., 98*, 430-438, 1984.

Torgeson, W. L., and S. C. Stern, An aircraft impactor for determining the size distributions of tropospheric aerosols, *J. Appl. Meteorol., 5*, 205-210, 1966.

Twomey, S., and K. N. McMaster, The production of condensation nuclei by crystallizing salt particles, *Tellus, 7*, 458-461, 1955.

Weber, R. J., P. H. McMurry, F. L. Eisele, and D. J. Tanner, Measurement of expected nucleation precursor species and 3 to 500 nm diameter particles at Mauna Loa Observatory, Hawaii, *J. Atmos. Sci., 52*, 2242-2257, 1995.

Wiedensohler, A., et al., Night-time formation and occurrence of new particles associated with orographic clouds, *Atmos. Environ., 31*, 2545-2559, 1997.

A. D. Clarke, J. Li, and M. Litchy, School of Ocean and Earth Science and Technology, University of Hawaii, Honolulu, HI 96822.

G. Kok and R. D. Schillawski, Research Aviation Facility, National Center for Atmospheric Research, Boulder, CO 80307.

P. H. McMurry, Particle Technology Laboratory, Department of Mechanical Engineering, University of Minnesota, Minneapolis, MN 44544.

R. J. Weber, Brookhaven National Laboratory, Department of Applied Science, Building 815E, P.O. Box 5000, Upton, NY 11973-5000. (email: rweber@bnl.gov)

(Received February 27, 1998; revised June 15, 1998;
accepted June 16, 1998.)